Int J Adv Manuf Technol (2012) 61:35–51
DOI 10.1007/s00170-011-3712-9

ORIGINAL ARTICLE

NURBS approximation to the flank-milled surface swept by a cylindrical NC tool

Chenggang Li · Sanjeev Bedi · Stephen Mann

Received: 1 May 2009 / Accepted: 18 October 2011 / Published online: 12 November 2011

Abstract In this paper, a method to approximate the flank-milled surface swept by a cylindrical cutter with a non-uniform rational basis spline (NURBS) surface is presented. The swept surface produced by the moving tool can be calculated as a collection of points organized as a series of grazing curves along the surface. The generated NURBS surface closely matches the grazing surface. The deviation between this surface and the grazing surface is calculated and is controlled by increasing the number of control points used to represent the surface.

Keywords Curved surface design · Flank milling · Surface numerical analysis · Surface error control

1 Flank milling

Flank milling is a widely used machining method in today's manufacturing industry. In flank milling, the side of the cutter machines the surface, removing the stock in front of it. Compared to other machining methods, flank milling can offer higher machining efficiency, higher material removal rate, and provide a better surface finish. Flank milling is used in the machining of turbine blades, fan impellers, and other engineering objects. Researchers working on improving flank milling have developed various tool positioning techniques in the past decade. In general, these techniques can be categorized into three classes, namely, direct tool positioning methods, step-by-step tool positioning methods and improved tool positioning methods.

In the direct tool positioning method, the cylindrical cutting tool is used to machine a ruled surface and the tool is positioned to be tangential to the given surface at one point on the ruled line either in the middle or end (or near the end) while the tool axis is parallel to the same ruled line. Alternatively, the tool is positioned to directly touch two points on the ruled line. The methods that belong to this class include early methods [1, 2], Rubio et al.'s method [1], Stute et al.'s method [3], Liu's method [4], etc. The error defined as the difference between the machined surface and the desired surface in this class is higher than errors from the classes described below, but the cutting tool is easy to position and the computation time of tool positioning is low.

A step-by-step tool positioning method is an improvement over the direct tool-positioning method. In this class, the cutting tool is first positioned on the given surface with one of the direct tool positioning methods and then the tool is lifted and/or twisted to reduce the error between the machined surface and the desired surface. Methods like those developed by Rehsteiner et al. [5], Bohez et al. [6], Tsay and Her [7], and Bedi et al. [8–11] belong to this class. In comparison to the direct tool positioning methods, the step-by-step tool positioning methods result in a machined surface that is close to the desired surface but the computation time of these methods is long.

An improved tool positioning method is a combination of the techniques used in the two classes described above. In this

C. Li · S. Bedi
Mechanical and Mechatronics Engineering Department,
University of Waterloo,
Ontario, Canada N2L3G1

C. Li
e-mail: cgli@engmail.uwaterloo.ca

S. Bedi
e-mail: sbedi@uwaterloo.ca

S. Mann (✉)
David R. Cheriton School of Computer Science,
University of Waterloo,
Ontario, Canada N2L3G1
e-mail: smann@uwaterloo.ca

method, the cutting tool is positioned on the given surface so that it touches at three contact points. A machined surface can be generated with many tool positions, each of which has three contact points (two on the guiding curves and one on the rule). Three contact points at any tool position can be obtained directly by solving seven transcendental equations based on the given geometrical conditions. The error between the machined surface and the desired surface is small in this type of tool positioning method. Redonnet et al.'s method [12] and Monies et al.'s method [13–15] belong to this class. This class of methods results in high accuracy machined surfaces. However, it requires the solution of seven transcendental equations at each tool position, which makes it computationally cumbersome.

All of the methods described above focus on ruled surfaces and attempt to use different techniques to reduce the deviation between the machined surface and the given surface. In spite of it being widely recognized that flank milling produces curved surfaces, no one has attempted to design free-form surfaces that can be flank milled with accuracy using no approximations. Some researchers, like Elber and Fish [16], Bohez et al. [6], tried to use flank milling techniques to machine free-form surfaces. In their methods, they first divide the target surface into multiple ruled surfaces, and then machine these ruled surfaces in pieces with one of the above techniques. Obviously, there are spatial limitations to this method and it results in long tool paths.

One of the key applications of flank milling is machining of impellers. Engineers design impeller surfaces to extract power from fluid flowing over them. Designers use sophisticated aerodynamic analysis to improve the efficiency and performance of impeller. However, to machine the impellers, these surfaces are approximated with ruled surfaces or produced at large cost with point machining techniques. Manufacturing engineers simplify the curved surface to a ruled surface to machine the part using flank milling even though a curved surface is better for efficiency and other requirements. If a curved surface that can be flank milled directly can be designed, it will be of great benefit not only for manufacturing but also for application engineering. With this surface design technique, engineers would be able to design impellers and optimize their performance without worrying about compromises during machining. How to achieve this goal is a big challenge in surface design and machining. In this paper, this challenge is probed and a solution is presented. First, the surfaces that can be machined with the flank milling method (by a cylindrical tool) are identified and then a method to design such surfaces is developed and tested.

The focus of this study is to develop a method to represent the machined surface with a non-uniform rational basis spline (NURBS) or B-spline representation so that the surface can be generated accurately by flank milling technique. Such a surface-fitting method can be used by engineers to design impellers and blades geometrically.

The key idea behind this method is to approximate the grazing surface with an NURBS definition based on the properties of guiding curves and the cylindrical cutter. At each tool position, the corresponding grazing curve lies on the cylindrical tool surface. When projected onto a plane perpendicular to the tool axis, this grazing curve becomes an arc and can be represented by an NURBS. The investigation shows that this NURBS can be constructed with three or four control points with their corresponding weights (as shown in Fig. 1). A method of moving these points off the plane along the tool axis direction is developed to accurately model the 3D grazing curve. As these control points (representing the grazing curve) are moved along guiding curves in a manner that nearly retains their grazing curve character, a surface is generated. This NURBS surface closely represents the grazing or swept surface and can be used in design.

Our method is similar to that of Yang and Abel-Malek [17], who gave an algorithm for approximating the swept volume of an NURBS solid. However, since we are focused on flank milling with a cylinder, our method is significantly simpler: we do not have to intersect a set of swept surfaces and the computation of points on the swept surface is simpler. Further, while they compute a volume, we only need compute a single swept surface to use for machining. Multiple tool passes with our method would need to intersect multiple swept surfaces, but Yang-Abel-Malek's method would have to intersect multiple swept volumes in addition to intersecting surfaces for each pass.

In the following sections, the proposed method is investigated and studied. In Section 2, the tool positioning method used to test the proposed solution, Bedi et al.'s

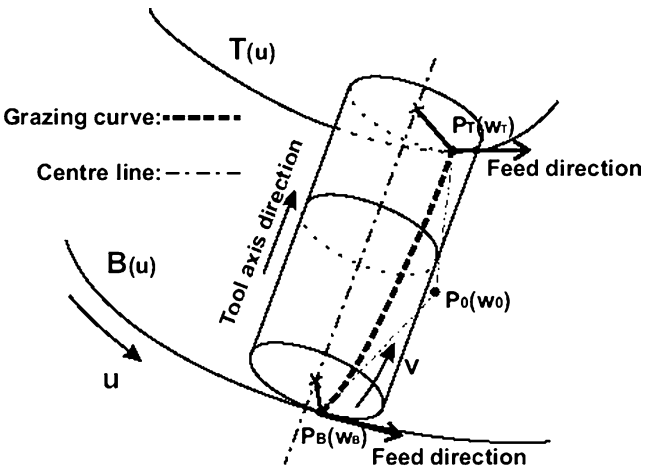

Fig. 1 The cylindrical tool and guiding curves: $T(u)$ and $B(u)$ are two guiding curves. P_T, P_0, and P_B are three control points of a grazing curve; w_T, w_0, and w_B are their corresponding weights. The tool moves along feed directions

method is given along with a method of computing the grazing surface (the swept surface) and a surface error measurement technique. Section 3 presents the strategy of modeling the grazing surface with NURBS definition. The basic theory of this method is developed. A flow chart to describe the implementation procedure is given in Section 4. Accuracy control of the surface design for flank milling with examples is discussed in Section 5. The proposed method is compared to the developed least square surface design method in Section 6. The paper is closed with the conclusion in Section 7.

2 Tool positioning method and swept surface

Different tool positioning methods result in different tool locations, orientations, and directions of motion for machining the same surface. Thus, a surface designed for flank milling will apply to a specific method of tool positioning. In this work, a surface design method is developed for designing a surface that can be flank milled. The tool positioning method developed by Bedi et al. [8–10] is applied to test the proposed method, although our method is general enough that it should be possible to use it with any tool positioning methods. A cylindrical tool is used in this study.

In addition to the tool positioning method, the surface design technique also depends on the actual shape of the surface produced by a moving tool. In previous work, the surface that is produced by flank milling has been evaluated. Bedi et al. [8] suggested a cross-product method to calculate the envelop surface. Mann et al. [18] generalized this method and applied it to tools with a general surface of revolution. The method evaluates the grazing surface (the swept surface) as a collection of discrete grazing points calculated using the cross-product method. Li et al. [10] and Menzel et al. [9] applied this method to conical and cylindrical tools to simulate the machined surface and used it to optimize each tool position. Li et al. [19] also used this method to study the surface error.

Lartigue et al. [20] presented a similar method to determine an envelop surface in their surface deformation analysis. Senatore et al. [21] used a similar method to define the grazing points and envelop surface. They also geometrically proved that, at each tool position, the contact points (between cutter and guiding curves, cutter, and rule) are on the envelop surface. All these techniques use discrete points to simulate the grazing surface (or the envelop surface). Furthermore, they use the grazing surface to approximate the machined surface. The accuracy of this approximation can be assessed with one of the error metrics used by different researchers [19]. The error metric used in this study is also described below.

2.1 Positioning a cylindrical tool on the surface

Based on Bedi et al.'s technique [8], a cylindrical cutter with radii R is positioned tangent to two curves at the same parameter value as shown in Fig. 2. The geometry of the tool and its relation to the guiding curves result in a set of simultaneous equations. When these equations are solved, the cutter position (P_T and P_B) at parameter value u can be obtained [8]. As the tool moves along the curves, it produces a swept surface.

2.2 The swept surface

A model of the swept surface is the basis of the proposed method. The swept surface is composed of grazing curves calculated at the various tool positions. After a tool position is defined, the grazing curve at each tool position can be derived using the cross-product method given in [8] and reviewed in the next paragraph.

As shown in Fig. 2 if the velocity at point P_T is V_T and at point P_B is V_B, then the velocity between P_B and P_T along tool axis direction can be linearly interpolated and is given by

$$V = V_B(1-v) + V_T v, \qquad 0 \le v \le 1 \tag{1}$$

The coordinate between P_B and P_T along the tool axis direction can also be linearly interpolated and is given by

$$P = P_B(1-v) + P_T v, \qquad 0 \le v \le 1 \tag{2}$$

The grazing curve between T and B is calculated as

$$G = P + \frac{V \times T_{\text{axis}}}{|V \times T_{\text{axis}}|} R \tag{3}$$

where, T_{axis} is the cutter axis direction.

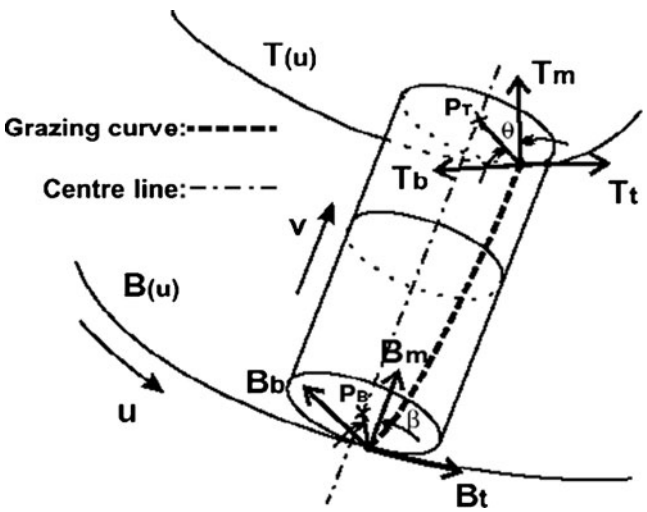

Fig. 2 Cutter rolling on two rails

Using Eq. 3, a continuous grazing curve can be obtained. For plotting, only a series of discrete grazing points are generated to represent the grazing curve. By connecting consecutive grazing curves along the u direction into a mesh, a swept surface (or a grazing surface) is generated. This surface represents the machined surface accurately. This surface is also composed of discrete points and does not have an exact NURBS representation. In engineering applications, an NURBS equation would be more helpful and acceptable especially when the target surface needs to be connected to other NURBS surfaces around it. Thus, to define a surface (with NURBS) that can be flank milled will be of significance in today's engineering applications.

2.3 The surface error measurement

To effectively evaluate the difference between the grazing surface and the approximate NURBS surface, an error metric is required. In the literature, different error measurement methods are used. In a previous work, these methods [19] were analyzed and compared. Generally, there are four types of error metrics used in the literature. These are the radial method, the parametric method, the tangent plane method and the closest point method. Even though these methods are designed for comparing the machined surface and the designed surface, they can also be used to measure the difference between the grazing surface (or a grazing curve) and the approximate NURBS surface (or an approximate NURBS curve) in surface design and are thus relevant to the context of this work.

If the grazing surface and the approximate surface are close, the two surfaces will nearly coincide and the errors from the different error measurement methods described above should be close or the same. In this work, the approximating NURBS surface and the grazing surface are usually close. However, under some circumstances, the parametric error method is not accurate enough for our work. Therefore, a modified parametric error measurement method will be used in this research to better reflect the surface error variation.

Figure 3 illustrates the modified parametric error measurement method. At each specific tool position, a grazing curve is calculated and plotted as the dash line. An NURBS curve is used to approximate the grazing curve. A plane perpendicular to the tool axis can be created. The two curves intersect the plane with two points, A and B. The distance between the A and the B is used as the approximating error at the grazing point A. We call this method as the *reparameterized parametric method* and will use it for error measurement in this paper.

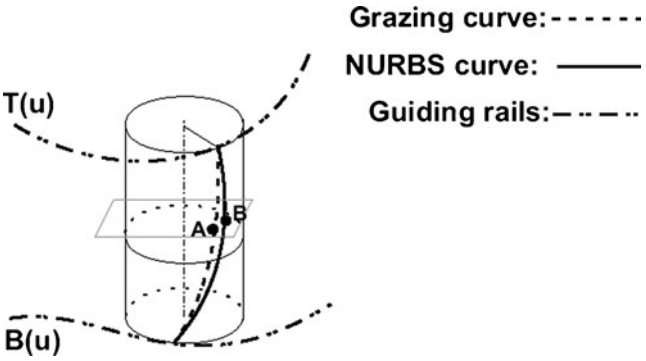

Fig. 3 A modified parametric error measurement method

3 NURBS approximating a swept surface

The idea behind the proposed technique for approximating a grazing surface is to select a few representative grazing curves and construct a surface that parametrically is close to these grazing curves. If enough grazing curves are used and they are close enough to one another, then the resulting surface should be a good approximation to the swept surface.

Each grazing curve is modeled using an NURBS representation (e.g., in Fig. 9, the control points $P_{0,0}$, $P_{1,0}$, $P_{2,0}$ are the NURBS representation for one grazing curve). Since we are working with a cylindrical tool, the projection of the grazing curve into a plane perpendicular to the tool axis direction will be a circular arc. Our approximation for the grazing curve starts with this circular arc, and then the control points are moved off the plane to form a good approximation to the grazing curve. A sequence of NURBS approximations to the grazing curves are used for several tool positions as the tool is moved along two guiding curves ($T(u)$ and $B(u)$ in Fig. 9). By increasing the number of control points along both the guiding curve and tool axis directions, better representations of grazing curves can be defined and a better NURBS approximation of the grazing surface can be obtained. The details of this method are presented below.

3.1 Approximating a grazing curve

The grazing curve is the contact between the grazing surface and the cutting tool. Thus, it lies on the cylindrical tool surface. This grazing curve is illustrated in Fig. 4 as a dashed line. This grazing curve can be approximated by a quadratic NURBS curve with control polygon $P_0P_1P_2$ shown as a solid line in Fig. 4, where P_0 is at the bottom of the guiding curve at $B(u)$ and P_2 is on the top guiding curve at $T(u)$. For simplicity, the coordinate system is setup at the bottom of the cylinder center with the Z axis lying along the cylinder axis. P_0 and P_2 have the same parameter value u along the guiding curves and are known;they also lie on the grazing curve. P_1 needs be determined. The

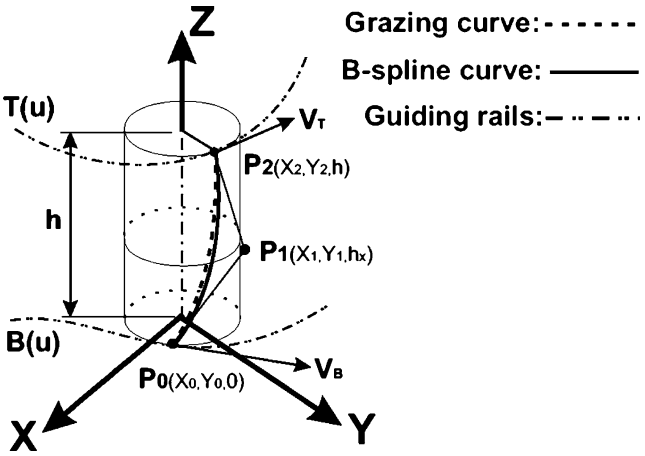

Fig. 4 Grazing curve and its control points on the cylindrical surface

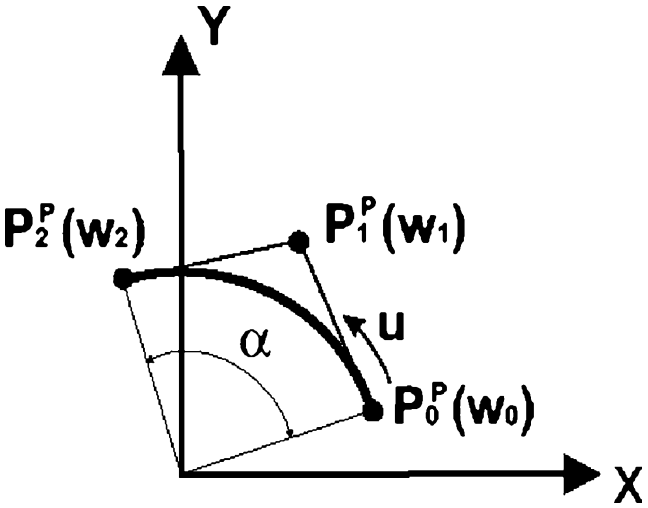

Fig. 5 Arc with its control points

grazing curve with the end points P_0 and P_2 is projected onto the x-y plane ($P_0{}^p$ and $P_2{}^p$ correspond to P_0 and P_2). This projected curve, $\overset{\frown}{P_0^p P_2^p}$, is a two-dimension arc and can be represented by a quadratic NURBS curve [22] with three weighted control points $P_0{}^p$, P_1^p and P_2^p. The X and Y coordinates of P_0^p and P_2^p are known; however, P_1^p needs to be calculated. P_1^p is calculated from the intersection of the two tangent lines passing through P_0^p and P_2^p. If α is the angle of the arc $\overset{\frown}{P_0^p P_2^p}$, then the weights w_0, w_1, and w_2 at points $P_0{}^p$, $P_1{}^p$, and $P_2{}^p$ are [22]:

$$w_0 = w_2 = 1,\ w_1 = \cos(\alpha/2)$$

Figure 5 shows this relationship graphically. The arc $\overset{\frown}{P_0^p P_2^p}$ can be represented exactly as a 2D NURBS curve $C^p(u)$ with control points P_0^p, P_1^p and P_2^p as

$$C^p(u) = \frac{(1-u)^2 w_0 P_0^p + 2u(1-u)w_1 P_1^p + u^2 w_2 P_2^p}{(1-u)^2 w_0 + 2u(1-u)w_1 + u^2 w_2} \quad . \quad (4)$$

3.1.1 Modeling of the grazing curve

Once the arc has been defined as a 2D NURBS curve, its control points can be stretched along the tool axis direction until P_0^p moves to P_0, P_2^p moves to P_2 and P_1^p moves to P_1, where P_1 needs to be decided. This changes the 2D NURBS curve of (5) to the 3D NURBS curve

$$C(u) = \frac{(1-u)^2 w_0 P_0 + 2u(1-u)w_1 P_1 + u^2 w_2 P_2}{(1-u)^2 w_0 + 2u(1-u)w_1 + u^2 w_2}. \quad (5)$$

The X and Y coordinates of P_1 are the same as P_1^p. The Z coordinate of P_1 must be properly selected to make the 3D NURBS curve closely match the grazing curve at this tool position.

The grazing curve is a function of the magnitude and direction of the velocities V_T and V_B as shown in Eqs. 1, 2, and 3. Since the Z coordinate of P_1 must be determined by measuring the deviation from the grazing curve, it becomes a function of V_T and V_B. A convenient assumption would be to assume $|V_T| = |V_B|$. This assumption will put P_1 in the middle of P_0 and P_2. The impact of this assumption on the error is studied in following section. Figure 4 shows this relationship graphically. The Z coordinates of P_0 and P_2 are 0 and h and P_0 and P_2 pass through the contact points $B(u)$ and $T(u)$, respectively.

3.1.2 Error in grazing curve ($|V_T| = |V_B|$)

If the Z coordinate of point P_1 is set to half of the effective contact length h (h_x=h/2, with h being measured along the tool axis direction between points P_0 and P_2), then the curve generated by Eq. 5 can be used to check the deviation of the grazing curve using the reparameterized parametric error measurement method described in Section 2.3. To check that the error in our approximation was small enough, we ran a test. For this test, the parameters of the cylindrical cutter and control points were

$$P_0[R\ \cos(\pi/6), R\ \sin(\pi/6).0], P_1\left[\frac{R\ \cos(\pi/4)}{\cos(\pi/12)}, \frac{R\ \sin(\pi/4)}{\cos(\pi/12)}, h/2\right]$$
$$P_2[R\ \cos(\pi/3), R\ \sin(\pi/3), h]$$
$$V_B[-R\ \sin(\pi/6),\ R\ \cos(\pi/6), 0], V_T[-R\ \sin(\pi/3),\ R\ \cos(\pi/3), 0]$$
$$w_0 = 1,\ w_1 = \cos(\pi/12), w_2 = 1,\ R = 10,\ h = 45$$

where, the X and Y coordinates of point P_1 are obtained using the method described in Section 3.1.1; R is the radii

of the cylindrical cutter; h is the effective contact length along the axis of the cylindrical cutter; V_B and V_T are velocities at points P_0 and P_2, their directions are along tangent line directions of each circle and their magnitudes are true velocities; w_0, w_1, and w_2 are the weights of points P_0, P_1, and P_2.

Using Eqs. 1, 2, 3, and 5, the grazing curve and the approximate NURBS curve can be obtained. The deviation between the two curves is calculated and is shown in Fig. 6. The errors at v=0, v=0.5, and v=1 are zero. The shape of the error curve is symmetric and the maximum error is smaller than 0.035 mm.

A close study of this error shows that the deviation between the NURBS curve and the grazing curve depends on the angle α between V_B and V_T which lie in the plane perpendicular to the tool axis, the radius of the cylindrical cutter, etc. The contact length (L) between the cutter and machined surface, however, has little influence on it. Different parametric combinations were considered and the resulting maximum deviations are listed in Tables 1, 2, and 3. From these tables, it can be seen that the influence of the angle α measured between V_B and V_T and the radii of the cutter are significant. The larger the angle α, the larger is the deviation; the bigger the radius, the bigger is the deviation (the deviation varies linearly to the tool radius). To effectively control the deviation, more control points can be used and curve tolerance requirement (the permitted error between the desired curve and the grazing curve) can be satisfied. In general, three control points satisfy most engineering applications for α<30° and R<30 mm.

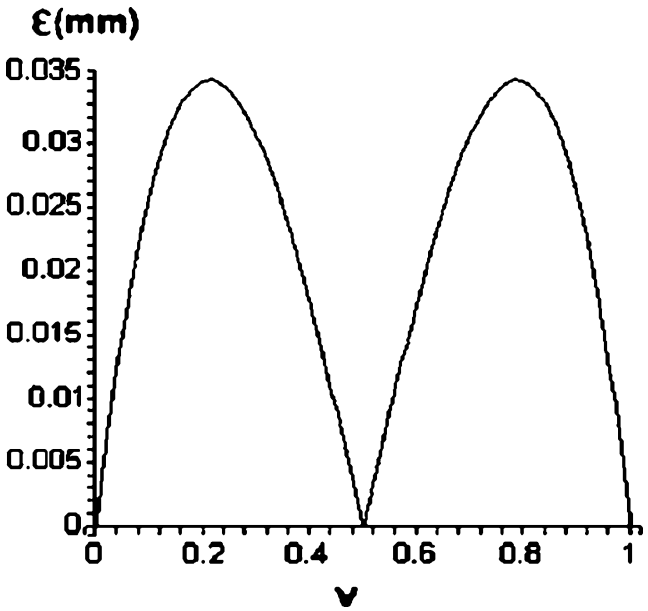

Fig. 6 Deviation along the grazing curve if $|V_B| = |V_T|$

Table 1 Max error for varying L (α=30°, R=10 mm)

L (mm)	25	45	65	85	105	150
ε (mm)	0.03493	0.03493	0.03493	0.03493	0.03493	0.03493

3.1.3 Modeling a grazing curve ($|V_T| \neq |V_B|$)

In a general situation, the magnitudes of velocities V_B and V_T are unlikely to be equal. The magnitude of V_B (or V_T) depends on the geometry of the guiding curves and the cutting tool. Different velocity magnitudes of V_B and V_T influence the velocity distribution along tool axis, and as a result affect the shape of the grazing curve. If the Z coordinate (h_x) of the middle control point P_1 is kept as h_x=h/2, the deviation between the given grazing curve and the approximate NURBS curve will increase. This is shown by considering the same example as before but where the magnitude of V_T is bigger than V_B ($|V_T|/|V_B| = 1.07$). The maximum deviation in this case is shown in Fig. 7 and is much bigger than the maximum deviation in Fig. 6.

To reduce the maximum deviation along the grazing curve, we moved the control point P_1 from the middle along the tool axis direction toward the point with the smaller velocity magnitude. By moving P_1 along the tool axis direction, we ensure that our approximation of the grazing curve will always lie on the surface of the cylindrical tool. The length of movement depends on the difference of the two magnitudes. The bigger the difference, the longer the movement. Our study shows that if the ratio between the two magnitudes is less than k=1.35 ($k = |V_B|/|V_T| \leq 1.35$ or $k = |V_T|/|V_B| \leq 1.35$), then the movement is less than or equal to $(k-1)h/2$. For the above example, P_1 was moved toward P_0 by 1.55 mm along the tool axis. The resulting deviation between the grazing curve and the approximation NURBS curve is significantly reduced as shown in Fig. 8.

If the ratio k is bigger than 1.35, moving the point P_1 does not reduce the maximum deviation enough to satisfy engineering requirement. In this case, four or more control points are needed to approximate the grazing curve. The simplest way to increase the number of control points is to use knot insertion [22].

If four or more control points are used, their locations along the axis of the tool are uncertain. These points are moved along the tool axis in a direction that reduces the deviation between the grazing curve and the approximate curve. Normally, four control points will satisfy require-

Table 2 Max error for varying α (L=45mm, R=10 mm)

α	10°	20°	30°	40°	50°	70°	90°
ε (mm)	0.001281	0.0103	0.0349	0.0835	0.165	0.467	1.033

Table 3 Max error for varying R (L=45 mm, α=30^0)

R (mm)	5	10	20	30	40	50
ε (mm)	0.0175	0.0349	0.0698	0.105	0.140	0.175

ments of normal engineering applications and produce surfaces that approximate the desired surface well.

3.2 Modeling of a surface

In the NURBS representation of the grazing curve, the outer control points move along two guiding curves $T(u)$ and $B(u)$ as explained in Section 2. To build an NURBS surface representation of the swept surface, we will make $T(u)$ and $B(u)$ be two of the boundaries of our NURBS surface. To do so, the two guiding curves, $T(u)$ and $B(u)$, must be constructed with the same number of control points. If the number of control points and the knot vectors are different for $T(u)$ and $B(u)$, then the method requires that additional control points be added to either or both $T(u)$ and $B(u)$ to ensure they have the same number of control points and knots.

Since $T(u)$ and $B(u)$ are the boundary curves of the grazing surface, the number of control points in the approximate NURBS surface along the generating lines should be equal to or greater than the number of control points in $T(u)$ (or $B(u)$). As an example, let the number of control points used to define $T(u)$ and $B(u)$ be three, and consider the case when the ratio of velocity magnitudes ($|V_B|/|V_T|$ or $|V_T|/|V_B|$) is less than 1.35, the angle α is less than 30° and tool radii is less than 30 mm. In the simplest case, we can choose the number of control points in the approximating NURBS surface along the guiding curve direction (u) to be three. Since each grazing curve is approximated by a three-control point NURBS curve, we can use three control points to define the approximating NURBS surface along the tool axis direction (v). A 3×3 NURBS surface can be created to approximate the grazing surface. The control points of this surface along with their weights are calculated using the technique given below. This new surface is comprised of a 3×3 grid of control point as shown in Fig. 9.

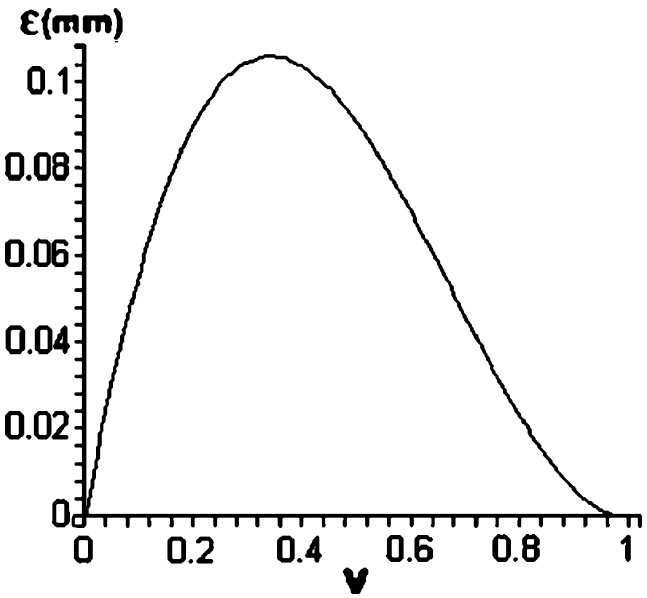

Fig. 7 Deviation along the grazing curve if $|V_T| \neq |V_B|$

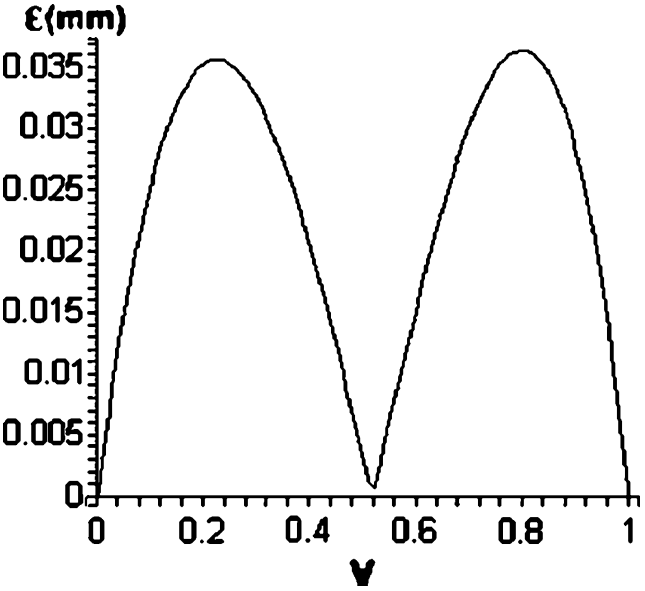

Fig. 8 Deviation after P_1 position shifting

Figure 9 shows the tool rolling along the quadratic guiding curves $T(u)$ and $B(u)$. The grazing curves at the start (u=0), the end (u=1) and the interior position (u=u_0) are shown as dashed lines. Each curve is approximated by an NURBS curve with three control points. The control points at u=0 and u=1 form the boundary of the control polygon of the approximate NURBS surface along the v direction; control points of the guiding curves form the boundary control points of the NURBS surface along the u direction. This leaves only one control point, $P_{1,1}$, undefined. The weights of the various control points also need to be determined.

3.2.1 Definition of NURBS function

An NURBS surface is defined as [22]

$$S(u,v) = \frac{\sum_{i=0}^{n}\sum_{j=0}^{m} N_{i,p}(v)N_{j,q}(u)w_{i,j}P_{i,j}}{\sum_{i=0}^{n}\sum_{j=0}^{m} N_{i,p}(v)N_{j,q}(u)w_{i,j}} \quad 0 \le u,v \le 1 \qquad (6)$$

where, m+1 and n+1 are the number of control points along u and v directions; $N_{i,p}$ and $N_{j,q}$ are the basis functions; p and

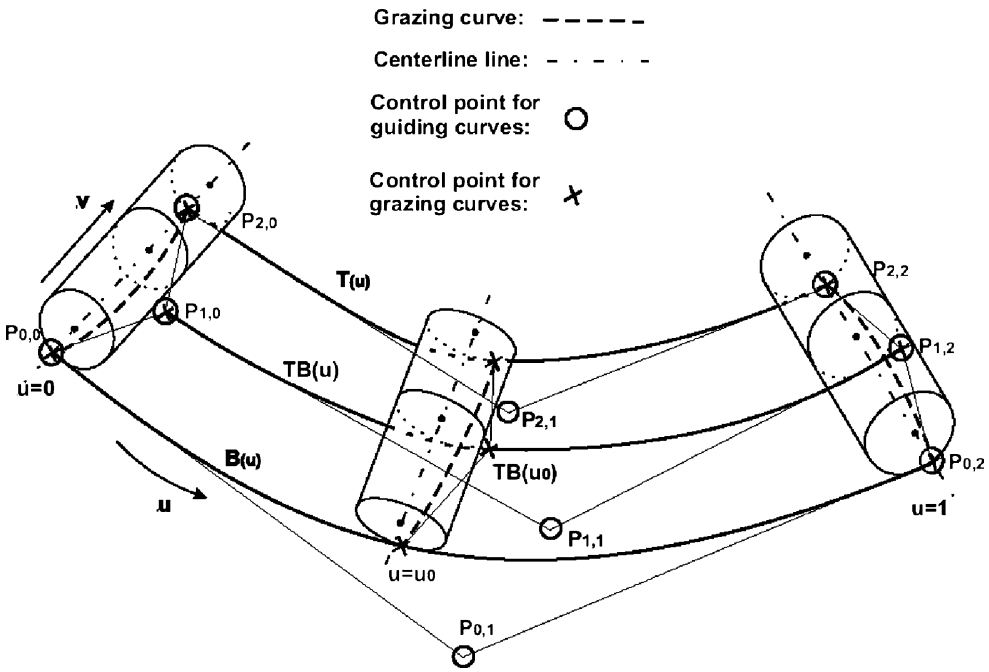

Fig. 9 Control points for approximate surface

q are the degree of the surface along v and u directions; $P_{i,j}$ are the control points and $w_{i,j}$ are the corresponding weights.

For a biquadratic surface with 3×3control points as shown in Fig. 9, Eq. 6 can be rewritten as

$$\begin{aligned} S(u,v) &= \frac{\sum_{i=0}^{2}\sum_{j=0}^{2} N_{i,2}(v)N_{j,2}(u)w_{i,j}P_{i,j}}{\sum_{i=0}^{2}\sum_{j=0}^{2} N_{i,2}(v)N_{j,2}(u)w_{i,j}} \\ &= \frac{N_{0,2}(v)\sum_{j=0}^{2} N_{j,2}(u)w_{0,j}P_{0,j} + N_{1,2}(v)\sum_{j=0}^{2} N_{j,2}(u)w_{1,j}P_{1,j} + N_{2,2}(v)\sum_{j=0}^{2} N_{j,2}(u)w_{2,j}P_{2,j}}{N_{0,2}(v)\sum_{j=0}^{2} N_{j,2}(u)w_{0,j} + N_{1,2}(v)\sum_{j=0}^{2} N_{j,2}(u)w_{1,j} + N_{2,2}(v)\sum_{j=0}^{2} N_{j,2}(u)w_{2,j}} \\ &= \frac{(1-v)^2 B^w(u) + 2v(1-v)TB^w(u) + v^2 T^w(u)}{(1-v)^2 w_B(u) + 2v(1-v)w_{TB}(u) + v^2 w_T(u)} \end{aligned} \tag{7}$$

where

$$T^w(u) = (1-u)^2 w_{2,0}P_{2,0} + 2u(1-u)w_{2,1}P_{2,1} + u^2 w_{2,2}P_{2,2} \tag{8}$$

$$TB^w(u) = (1-u)^2 w_{1,0}P_{1,0} + 2u(1-u)w_{1,1}P_{1,1} + u^2 w_{1,2}P_{1,2} \tag{9}$$

$$B^w(u) = (1-u)^2 w_{0,0}P_{0,0} + 2u(1-u)w_{0,1}P_{0,1} + u^2 w_{0,2}P_{0,2} \tag{10}$$

$$w_T(u) = (1-u)^2 w_{2,0} + 2u(1-u)w_{2,1} + u^2 w_{2,2} \tag{11}$$

$$w_{TB}(u) = (1-u)^2 w_{1,0} + 2u(1-u)w_{1,1} + u^2 w_{1,2} \tag{12}$$

$$w_B(u) = (1-u)^2 w_{0,0} + 2u(1-u)w_{0,1} + u^2 w_{0,2} \tag{13}$$

In Eq. 7, each specific u value represents a grazing curve. This grazing curve is approximated by an NURBS curve with three control points $T^w(u)$, $TB^w(u)$, and $B^w(u)$. $T^w(u)$ is the homogeneous coordinates of $T(u)$. It can be written as

$$T^w(u) = T(u) \cdot w_T(u)$$

where, $w_T(u)$ is its corresponding weight.

Similarly,

$$TB^w(u) = TB(u) \cdot w_{TB}(u),\ B^w(u) = B(u) \cdot w_B(u)$$

For polynomial guiding curves, the weights of control points $w_{2,0}$, $w_{2,1}$, $w_{2,2}$, $w_{0,0}$, $w_{0,1}$, and $w_{0,2}$ are equal to 1. Equation 7 can be rewritten as

$$S(u,v) = \frac{(1-v)^2 B(u) + 2v(1-v)TB^w(u) + v^2 T(u)}{(1-v)^2 + 2v(1-v)w_{TB} + v^2} \quad (14)$$

where

$$T(u) = (1-u)^2 P_{2,0} + 2u(1-u)P_{2,1} + u^2 P_{2,2} \quad (15)$$

$$B(u) = (1-u)^2 P_{0,0} + 2u(1-u)P_{0,1} + u^2 P_{0,2} \quad (16)$$

There are two unknown vectors in Eq. 14, $TB^w(u)$ and w_{TB}. Between $TB^w(u)$ and w_{TB} (Eqs. 9 and 12), six unknowns, $P_{1,0}$, $w_{1,0}$, $w_{1,1}$, $P_{1,1}$, $w_{1,2}$, and $P_{1,2}$, need to be determined.

At u=0, Eq. 14 simplifies to the grazing curve at the start point of the guiding curves. Since the equation of the grazing curve and its NURBS curve approximation (see Section 3.1) are known, $P_{1,0}$ and $w_{1,0}$ can be determined.

Similarly, at u=1, Eq. 14 simplifies to the grazing curve at the end of the grazing surface. Equating it to the approximate NURBS surface results in $P_{1,2}$ and $w_{1,2}$. The remaining two unknowns, $P_{1,1}$ and $w_{1,1}$, can also be calculated correspondingly; however, in this case, the grazing curve at $u=u_0$ is used.

Various methods can be used to select u_0; we used a uniform step method, which in this case sets u_0=0.5. Depending on the data, another method such as chord length [22] could be used. Once u_0 is decided, w_{TB} can be set to $w_{TB} = \cos\alpha_3/2$, where α_3 is the angle between $B(u_0)$ and $T(u_0)$ measured in the plane normal to the cylinder axis. Equations 14, 12, and 9 can be solved for $w_{1,1}$ and $P_{1,1}$.

If the guiding curves have more than three control points, additional grazing curves at $u=u_i$ may be required. Each grazing curve is used to determine two unknown coefficients.

3.2.2 Re-evaluation of weight

Even though $w_{1,1}$ and $P_{1,1}$ can be calculated by Eqs. 14, 12, and 9, the weights and control points used in the equations will not result in a good approximating NURBS surface because $w_{1,0}$, $w_{1,2}$, and w_{TB} are obtained by considering the grazing surface shape along the tool axis direction (the v direction) but the shape of the grazing surface along the feed direction (the u direction) is not considered. This results in surface error between the approximate surface and the grazing surface. Thus, to effectively control the surface error, the weight selection should reflect the change in shape of the grazing surface not only along the tool axis direction, but also along the feed direction. More control points can be added along the feed direction to reduce this error. With an increase in the number of the control points along the feed direction, the error of the approximating NURBS surface can be effectively controlled. This will be discussed in Section 5. Another solution is to determine the weight of the middle control point in a way that takes into account the surface variation along the guiding curves. An average weight can be used to roughly reflect the surface shape variation along the feed direction. Hence, the weight of the middle control point is set to the average weight of all the interior control points as shown below:

$$\begin{aligned} w^* &= (w_{1,0} + w^{TB} + w_{1,2})/3, \\ \overline{w}_{1,0} &= \overline{w}_{1,1} = \overline{w}_{1,2} = w^{TB} = w^*, \end{aligned} \quad (17)$$

where, $w_{1,0}$,w^{TB} and $w_{1,2}$ are corresponding interior control point weight of each grazing curve at three tool positions and $\overline{w}_{1,0}$, $\overline{w}_{1,1}$ and $\overline{w}_{1,2}$ stand for the weights of interior control points of the approximating NURBS surface. When an NURBS surface is created using this method, it results in a smaller maximum surface error as compared to the surface with variable weights $w_{1,0}$, w^{TB} and $w_{1,2}$. We are unsure to why averaging gives smaller error, but we mention this since it gives better results. This will be discussed in Sections 5.2.1 and 5.2.2. Substituting the result of Eq. 17 into Eq. 9, $P_{1,1}$ is determined. Once all the unknowns are solved, Eq. 14 gives the approximating NURBS surface.

3.2.3 Generalization of surface modeling

The guiding curves $T(u)$ and $B(u)$ can have more than three control points. Suppose that the guiding curves $T(u)$ and $B(u)$ are two NURBS curves of degree p, then the degree of the approximating NURBS surface along the feed direction can be selected to be p as well. The number of control points along the feed direction will be n+1, where $n \geq p$. The control points of the NURBS surface in the tool axis direction can still be 3. If there are n+1 control points along the guiding curve direction, then n+1 tool positions are used to determine the NURBS surface.

At each of these tool position, the grazing curves are developed and the NURBS approximation to these curves are used to calculate the weights $k_0, k_1, k_2, \ldots, k_n$ at the interior control points. While we could use the weights $k_0, k_1, k_2, \ldots, k_n$ directly, we again found that averaging the weights gives better results. The equations to compute these weights are given below (Fig. 10).

$$\begin{aligned} w_i &= \sum_{j=0}^{p} (k_{i+j} + k_i)/(2(p+1)), && \text{if } 0 \leq i \leq p \\ w_i &= \sum_{j=0}^{p} (k_{i+j} + k_{i-p+j})/(2(p+1)), && \text{if } p < i < n-p \\ w_i &= \sum_{j=0}^{p} (k_{n-p+j} + k_{i-p+j})/(2(p+1)), && \text{if } n-p \leq i \leq n \end{aligned} \quad (18)$$

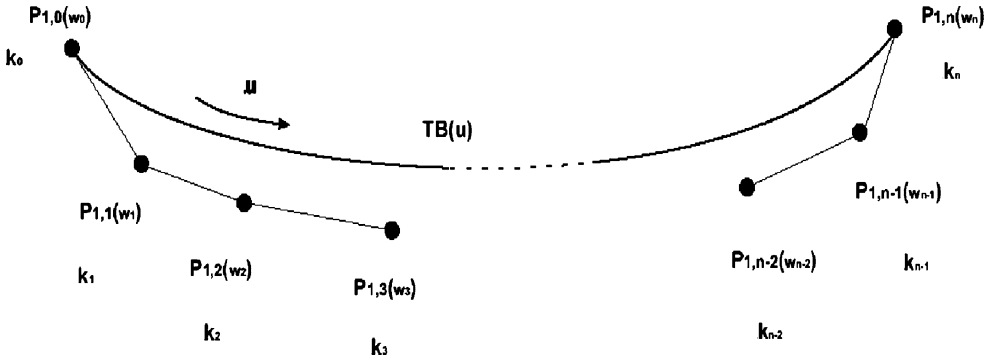

Fig. 10 Weight distribution along $TB(u)$

With these weights, NURBS equations of the grazing curves in terms of the unknown control points [22] can be obtained as

$$\begin{aligned} TB(u_1) &= \frac{\sum_{i=0}^{n} N_{i,p}(u_1)P_{1,i}w_i}{\sum_{i=0}^{n} N_{i,p}(u_1)w_i} \\ TB(u_2) &= \frac{\sum_{i=0}^{n} N_{i,p}(u_2)P_{1,i}w_i}{\sum_{i=0}^{n} N_{i,p}(u_2)w_i,} \\ &\vdots \\ TB(u_{n-1}) &= \frac{\sum_{i=0}^{n} N_{i,p}(u_{n-1})P_{1,i}w_i}{\sum_{i=0}^{n} N_{i,p}(u_{n-1})w_i} \end{aligned} \tag{19}$$

These equations can be solved for the interior control points ($P_{1,i}$, $i = 1, \cdots, n-1$) of the approximate NURBS surface. With these control points and their corresponding weights, the approximate surface is completely defined.

After the surface is defined, the deviation between the actual grazing surface and the approximate NURBS surface can be evaluated using the error measurement methods described in Section 2.3. Control points of the NURBS surface can be increased along the u and/or the v direction if the surface error is more than the specified tolerance. The knot insertion method can be used to increase control points in the u and/or the v direction. With more control points, the surface deviation can be lowered but more unknowns need to be calculated. The calculation procedures, however, are the same as above.

4 Flow chart for surface design

To explain the basic concept of surface design for flank milling, a flow chart that describes the whole design procedure is given in Fig. 11. This chart can also be used to implement the surface design process.

The design starts with two user-specified guiding curves and their control points. The cutting tool is also selected by the user at the onset of design. Depending on the relationship among the grazing surface, the cutting tool and the guiding curves, the number of control points and the knot vector of the approximate NURBS surface can initially be determined. Consequently, the average weight of interior control points can be calculated.

In the proposed method, the position of the interior control point is initially set to the middle of each effective tool contact length at all specified tool positions. The positions of these interior control points are then optimized to reduce the error over the whole design surface. After optimization, all control points of the flank millable surface are known and this flank millable surface can be built. The

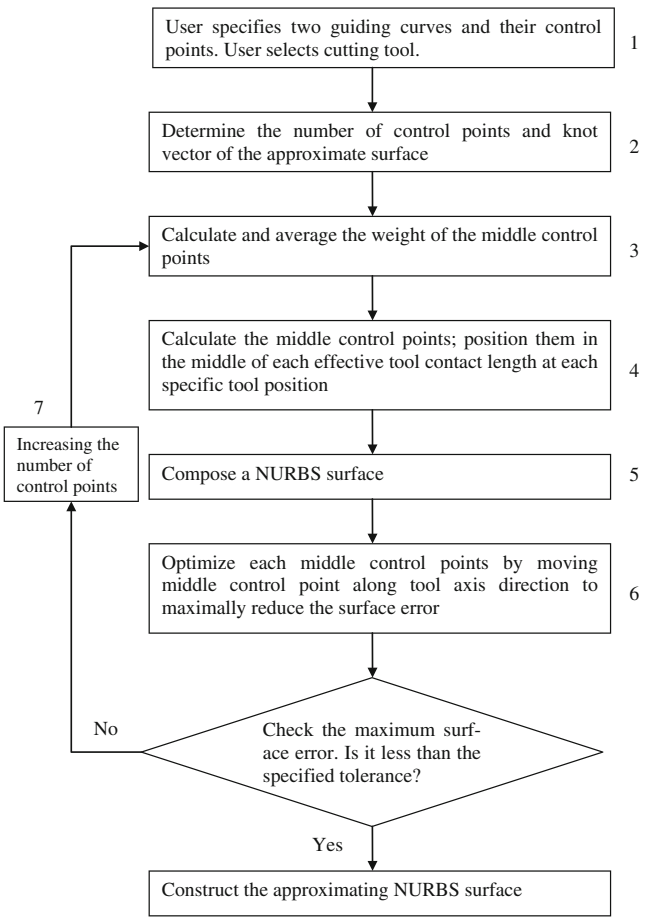

Fig. 11 The flow chart of implementation

error that would result when this surface is machined is checked next. If the maximum surface error exceeds the specified tolerance, more control points can be added to the control polygon of the surface and this process is iterated until the surface error reaches the required tolerance.

5 Accuracy control for surface design

In this section, the technique of designing a surface for flank milling is demonstrated with examples and the method to control the surface error in the design of the flank millable surface is also studied. The results are explained by referring to the flow chart shown in Fig. 11.

In the flow chart, the step to optimize the middle control points along the tool axis direction is performed as part of generation of the approximating NURBS surface. This is different from the method given in Section 3. In Section 3, the optimization of the middle control point is performed before the flank millable surface is constructed in step 5. As the middle control point for each tool position is optimized separately, the influence from other grazing curves is not considered. A study of the effect of optimizing the location of the middle control points on the overall surface error was done. The study shows that reducing the maximum error between the grazing curve and the approximating NURBS curve does not necessarily reduce the maximum surface error between the flank millable surface and the grazing surface.

As illustrated in Fig. 12, as the middle control point of the first approximating curve changes, the maximum error between the approximating NURBS curve and the grazing curve can reduce while the maximum error between the flank millable surface and the grazing surface increases. To avoid this, a new method to optimize the middle control point is employed. In this new method, the middle control points of all selected grazing curves are moved together as the surface error is optimized. The middle control points are thus located to optimize for minimal surface error.

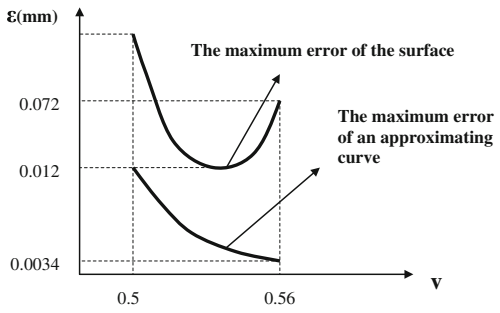

Fig. 12 The maximum error of the grazing curve and the grazing surface as middle control point moved along tool axis direction to reduce the grazing curve error

5.1 Surface design for flank milling

The design of a surface that can be flank milled begins with two guiding curves, $T(u)$ and $B(u)$. In our example, the two quadratic curves represent the top and the bottom curves of an impeller or a blade surface. The control points for the curves are tabulated in Table 4. The degree of both the curves is 2. The knot vector of the two curves is [0, 0, 0, 1, 1, 1].

An NURBS surface that can be accurately flank milled is designed. A cylindrical cutter of radius R=5 is used and Bedi et al.'s tool positioning method is adopted to position the cutter and consequently to generate the tool path. The resulting machined surface is calculated using the swept surface method. The grazing surface and the guiding curves are plotted in Fig. 13.

The first step in designing the NURBS surface is to select the number of control points of the surface and its knot vector. The control points and knot vector are selected by the user. Since the guiding curves lie on the machined surface and the numbers of control points defining the guiding curves in this example are three, the numbers of control point of the design surface along the guiding curve direction can initially be selected to be three. The knot vector of the surface along the guiding curve direction is the same as the guiding curve, i.e., [0, 0, 0, 1, 1, 1]. These parameters can be corrected based on the surface error analysis later. If the maximum surface error is larger than the specific tolerance, more control points can be added with a corresponding change in the knot.

In the second step, the tangent vectors of $T(u)$ and $B(u)$, that represent the direction of motion of the tool at these points, are investigated by plotting the angle α, which is the angle between the tangent vectors of $T(u)$ and $B(u)$ measured in the plane perpendicular to the cutting tool axis. The angle α and the ratio of the magnitudes of these tangents "k" are plotted as shown in Figs. 14 and 15. The angle α varies from 24° to 28.1°, the ratio k changes from 0.89 to 1.12. Since the magnitude does not change radically, three control points will be used to model the approximating surface along the tool axis direction. Experiments with different surfaces have shown that if the ratio k is bigger than 1.35 (or smaller than 0.74) or the angle α is bigger than 30°, then more control points should be used in the tool axis direction.

Table 4 Control points for guiding curves [mm]

	T0	T1	T2	B0	B1	B2
x	75	30	0	60	30	15
y	15	30	60	0	30	75
z	−5	−5	−5	−45	−45	−45
w (weight)	1	1	1	1	1	1

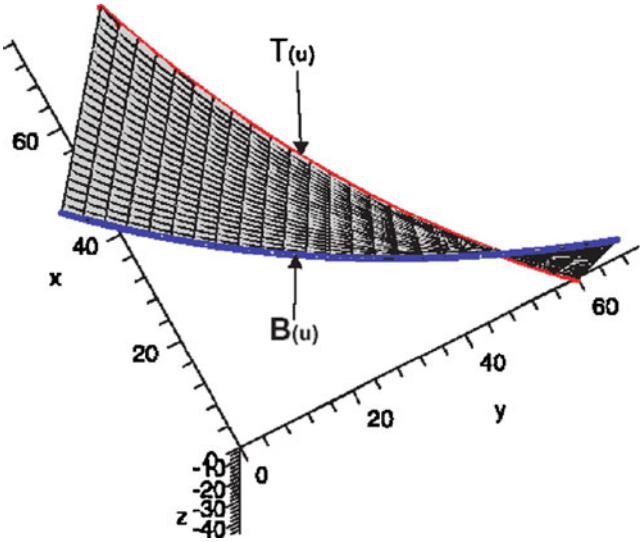

Fig. 13 The grazing surface and guiding curves

In the third step, a 3×3 biquadratic NURBS surface is constructed using the proposed surface design method. The procedure to build this surface is demonstrated in the next section.

5.2 Three by three approximate NURBS surface

Blocks 3–6 in Fig. 11 are used in this section. The control points and weights of the generating curves are directly assigned to the corresponding control points of the surface. This leaves three of the middle control points, namely $P_{1,0}$, $P_{1,1}$, and $P_{1,2}$, and their corresponding weights undetermined (see Fig. 9). The middle control points and weights

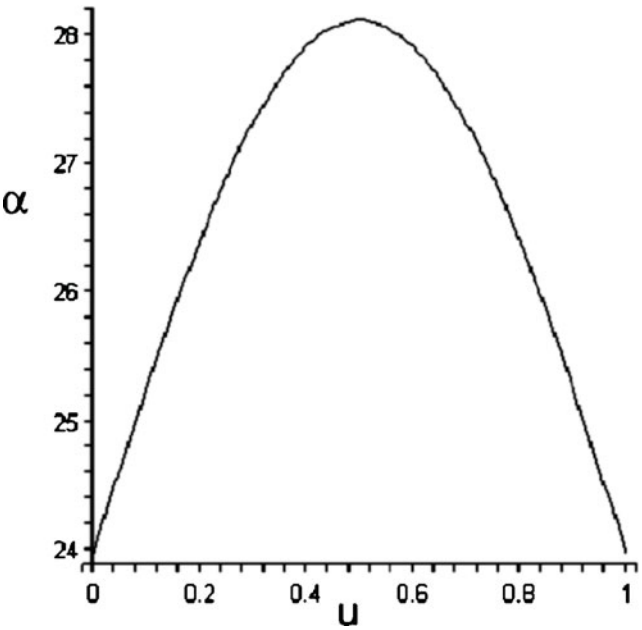

Fig. 14 The variation of angle α along the feed direction

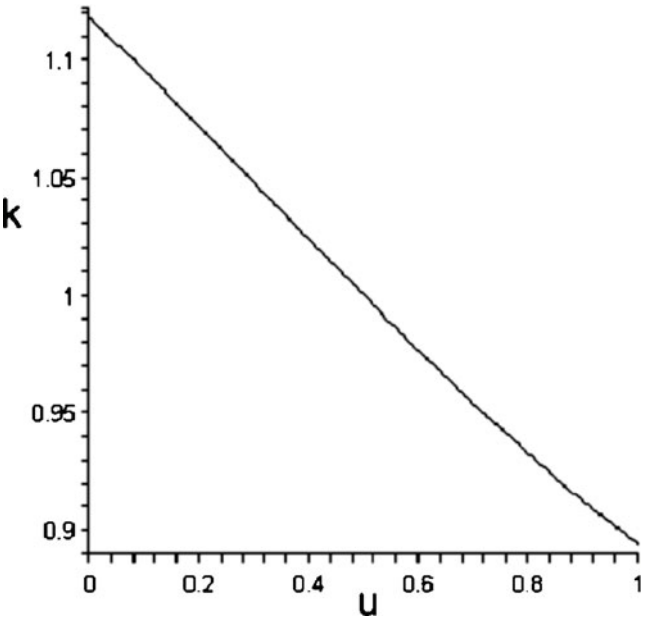

Fig. 15 The variation of the ratio k along the feed direction

are defined with the method discussed in Section 3. Three tool positions, u=0, u=0.5, and u=1, are used to decide these parameters. At each specified tool position, a grazing curve is calculated, then an NURBS curve is used to approximate this grazing curve. The middle control points of the NURBS curves are optimized together by moving their locations simultaneously to reduce the approximate NURBS surface error as explained in Section 4. The middle control points of the NURBS curve at tool positions u=0 and u=1 are directly added to the control polygon of the surface. The remaining control point $P_{1,1}$ is calculated as described in Section 3. The weights of these middle control points were determined when the grazing curves were calculated. These weights are averaged and re-assigned to the middle control points. After all control points and weights are obtained, a 3×3 NURBS surface is generated. The reparameterized parametric error measurement method is used to measure the deviation between the grazing surface and the designed NURBS surface. The result is shown in Fig. 16.

The deviation between the grazing surface and the approximate surface is in the range [0, 0.022]. The maximum error is less than 0.022. In generating this surface, the velocity at the top and the bottom were assumed to be given by the derivatives of $T(u)$ and $B(u)$. Similarly, the weights of the middle control points were averaged. The effect of these assumption (or steps) is explored next before the method of improving surface error is presented.

5.2.1 Surface model for fixed middle control point (v= 0.5)

The selection of the middle control points is based on the ratio of the velocity magnitudes at $T(u)$ and $B(u)$. For

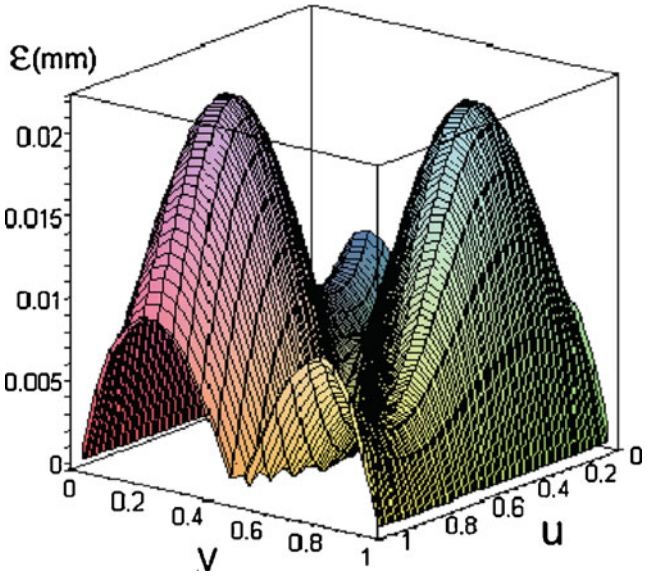

Fig. 16 Deviation between the grazing surface and the NURBS surface

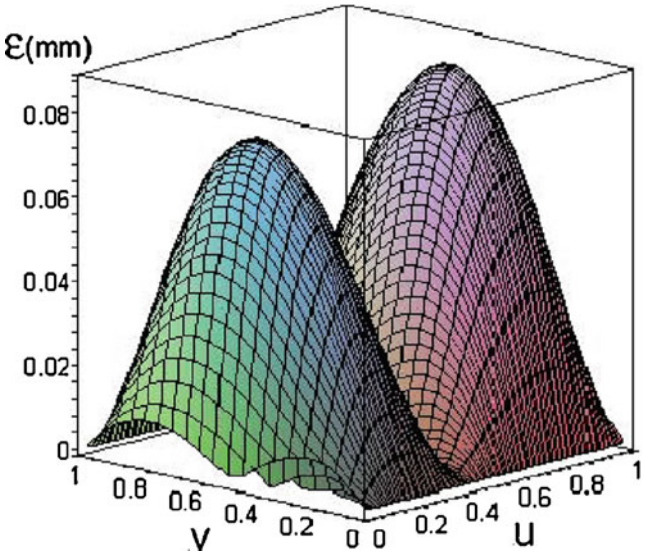

Fig. 18 Deviation between the grazing surface and the NURBS surface with separate weight of each middle control point

simplification, this ratio can be neglected and the middle control point (along $TB(u)$, see Fig. 9) is forced to lie at v= 0.5, the middle of the effective contact length along the tool axis. This will simplify the procedure and speed up the computations. But this changes the NURBS surface. Following the flow chart steps 1–5 (Fig. 11), the flank millable surface is reconstructed and the deviation is again measured and the result is plotted in Fig. 17.

The deviation between the grazing surface and the approximate surface using the fixed middle control point is in the range [0, 0.045]. The maximum deviation is close to 0.045. Compared to Fig. 16, the maximum deviation has increased, but the surface design procedure is simpler. The middle control points are obtained easily. This deviation may be acceptable in some engineering situation especially when the ratio of velocity magnitudes (between two contact points on $T(u)$ and $B(u)$) is close to 1 and further improvement can be achieved by insertion of knots or degree elevation as described later. If the ratio of magnitudes is equal to 1, Figs. 16 and 17 will give similar results.

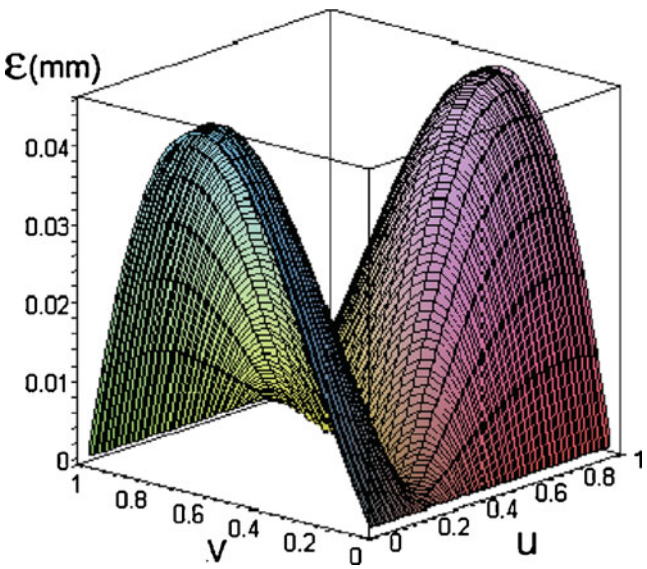

Fig. 17 Deviation between the grazing surface and the NURBS surface with a fixed middle control point

5.2.2 Effect of varying weight on surface model

The results obtained above use the average weight for each middle control point of the NURBS surface. If separate weights are used for each middle control point as described in Section 3, our algorithm follows the path 1, 2, 4, 5, and 6 in the flow chart in Fig. 11 resulting a different surface. The error of this surface is plotted in Fig. 18.

The deviation between the grazing surface and the approximate surface is in the range [0, 0.088]. The maximum deviation is close to 0.088. Compared to Fig. 16, this gives a larger deviation. The separate weight of each middle control point results in a highest surface error in all the cases tried by authors. Thus, we recommend using weights that are the average of the weights from the NURBS grazing curves are used.

Table 5 Errors for different NURBS surface (*CPs* control points)

CPs ($v\times u$)	3×3	3×4	3×5	4×3	4×4	4×5
ε_{max}	0.022	0.0195	0.0165	0.0152	0.0087	0.0065

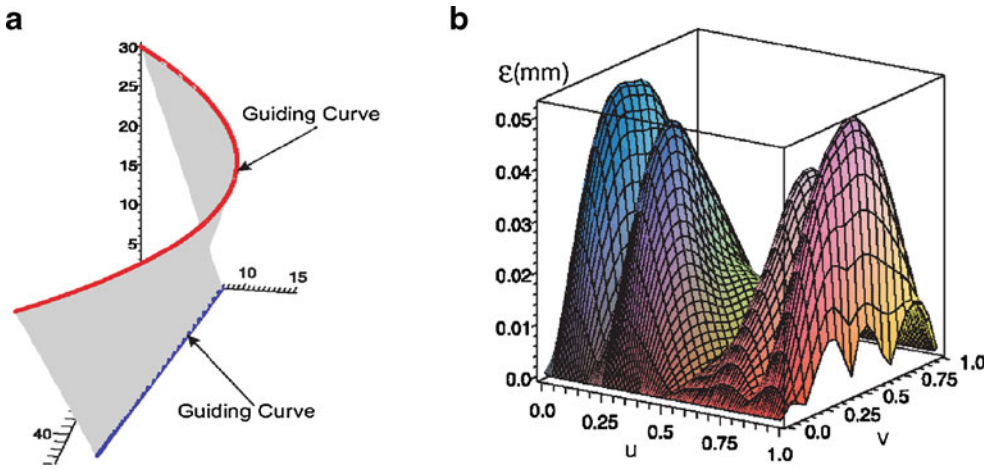

Fig. 19 The surface designed using the proposed method and its surface error. **a** The designed surface and its guiding curves. **b** The surface error distribution

5.3 Flank millable surface with more control points

As discussed before, the deviation between the grazing surface and the flank millable surface will decrease if the control points along the generating curve direction (u) and/or along the tool axis direction (v) are increased. To illustrate this, additional control points are added to the surface generated in the example above.

5.3.1 Increasing control points in the u and/or v direction

In this case study, the numbers of control points along v or the tool axis are kept the same. The control points in u direction or along the guiding curves are increased from three to four and then to five. Knot insertion [22] is used to increase the number of control points. The degree of the NURBS surface is kept the same, i.e., two. The control points of the two guiding curves ($T(u)$ and $B(u)$) are first increased, then, the remaining control points and weights along the middle are decided. For four control points, the knot vector becomes $[0,0,0,\frac{1}{2},1,1,1]$ and four tool positions, at u=0, u=0.33, u=0.66 and u=1, are used to calculate the middle control points and weights. For the case of five control points, the knot vector becomes $[0,0,0,0,\frac{1}{3},\frac{2}{3},1,1,1]$ and five tool positions, u=0, u=0.25, u=0.5, u=0.75, and u=1, are used to calculated the middle control points and weights. Using the technique developed above, the approximating NURBS surfaces are created and the surface deviations are calculated and listed in Table 5.

Similarly, one can increase control points in v direction and keep the number of control points in u direction the same. A quadratic NURBS surface is created for several sets of control points and the surface error is calculated and also tabulated in Table 5.

In general, the maximum surface error decreases with the number of control points increased in the v direction. The control points can also be simultaneously increased in both u and v directions to further reduce the deviation between the grazing surface and the NURBS surface. From Table 5, it can also be seen that the maximum surface errors are reduced insignificantly as the numbers of control points are

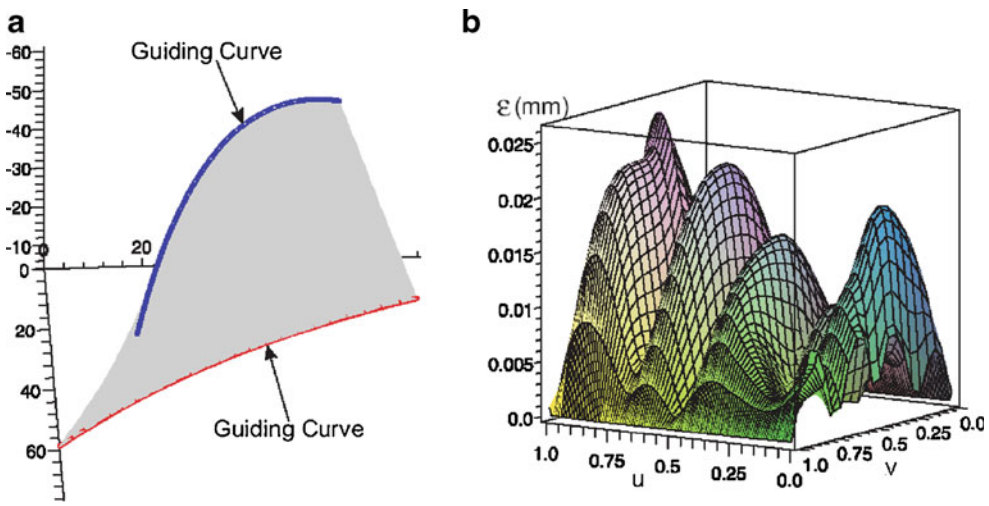

Fig. 20 The surface designed using the proposed method and its surface error. **a** The designed surface and its guiding curves. **b** The surface error distribution

Table 6 Error comparisons [mm]

Reference name	Ruled surface 1 (original tool position)	NURBS surface (original tool position)	NURBS surface (original tool position) (6×9)	Ruled surface 2 (optimizing tool position)
Example 1 (Fig. 16)	−0.15, 0	0.022 (3×3)	0.00156	−0.01, 0.0063
Example 2 Fig. 19	−0.32, 0	0.053 (4×5)	0.0097	−0.025, 0.02
Example 3 Fig. 20	−0.32, 0	0.026 (4×5)	0.0091	−0.022, 0.012

only increased in the u direction from 3×3 to 3×4 and 3×5. However, the maximum surface errors are reduced drastically when the numbers of control points are increased in both of u and v directions. It suggests that both of u and v directions need to be considered when the control points are added to the control net of the surface. Sometimes, adding control points in only one direction does not significantly reduce the maximum surface error.

5.4 Additional examples

The proposed method was also tried on two more examples of different surfaces as demonstrated below. The deviation of the surface in both examples can be effectively controlled by changing the number of control points and the knot vector. The guiding curves used in surface design are shown in Figs. 19a and 20a as bold lines. The error distribution calculated with the method described earlier is given in Figs. 19b and 20b for the respective surfaces. The desired of the approximating surface can be achieved in each case with increase in control points.

We have also used one of our methods to design an impeller as detailed in [23]. In our examples, we move the tool along the guiding curves so that the tool is tangent to one point on each guiding curve at the same parameter value u and we consider the resulting swept surface. Our method is a better approximation to this swept surface than a ruled surface is. However, if we wanted to machine a ruled surface, we could optimize the tool position so that the resulting swept surface minimized the error to a ruled surface.

Table 6 gives a comparison of the errors for different methods. Column 1 gives the error in approximating the swept surface with a ruled surface, where the swept surface is the surface swept by keeping the tool tangent to $T(u)$ and $B(u)$; from the table, we can see that a ruled surface is a poor approximation to the swept surface. Column 2 gives the error between our method and the swept surface, which is an order of magnitude improvement over ruled surface; the numbers in parentheses in this column indicate the number of control points used by our method.

Column 4 gives the error between a ruled surface and a method optimized to minimize the error between the swept surface and a ruled surface. We first note that the errors are similar in magnitude in columns 2 and 4. However, it should also be noted that the method for minimizing the error to the ruled surface can not be improved for a single pass of the tool: there are limits in how accurately the swept surface can approximate a ruled surface. On the other hand, with our method for approximating the swept surface, if the error is too high, then a better NURBS approximation to the swept surface can be constructed. Column 3 of this table shows the error resulting when using a 6×9 NURBS surface to approximate the swept surface. As can be seen from the table, the error has been reduced by one order of magnitude in all the examples. Further reductions in error can be obtained by further increasing the number of control points.

6 Comparison with the least square method

This paper presents a method for design of a flank millable surface that approximates the grazing surface. Although the accuracy of the approximation can be improved by knot insertion, we would like to compares its accuracy with the established least square technique, which guarantees the best fit. In the least square method, an approximate curve or surface can be obtained for a given set of sample points based on the degree and the knots vector specified by the user. Sample points should be spread out over the entire surface and the method requires matrix inversion in its computation.

The example given in Section 5.1 is used to design a flank millable surface with the least square method. Grazing points are used as sample points. Different quadratic NURBS approximating surfaces are obtained based on the number of user specified control points used in the computation. The resulting flank millable surfaces are compared with the grazing surface using the parametric error measurement method and the final results are shown

Table 7 The maximum error (mm) in the flank millable surfaces generated using different number of control points

CPs methods	3×3	3×4	3×5	4×3	4×4	4×5
LS	0.016	0.013	0.0134	0.0108	0.0045	0.0025
PM	0.022	0.0195	0.0165	0.0152	0.0087	0.0065

CPs Control points, *LS* least square, *PM* proposed method

in Table 7 below. The results from the proposed method are also listed in this table.

From this table, it can be seen that the maximum errors from different surface fitting methods are in the same range. The least square method offers a higher accuracy surface for the same number of control points, etc., but the error is dependent on the selection of knot vector, the parametric value of each sample point, the number of sample points and their distribution. Furthermore, the computation process is complex and time consuming. On the other hand, the surface error from the proposed method is not influenced by the variation of the number of sample points. The knot vector of the surface is the same as the knot vector of the guiding curves. The parametric value of each sample points is known. Only a few tool positions are used to define the approximating surface. The computation process is simple and computation time is short and the flank millable surface error can be controlled by increasing the number of control points of the surface.

7 Conclusion

In this paper, a method to design a surface for flank milling is developed. The discrete grazing points on the grazing surface at a few tool positions are used to decide the control points (and their weights) and to determine the approximate NURBS surface. This NURBS surface is desirable for flank milling as it can be machined precisely. The simulation results show that the error between the grazing surface (the simulated machined surface) and the approximate NURBS surface are small and satisfy the requirement of most engineering applications. If higher accuracy is required, the method allows additional control points to be added. The parameters affect the surface design are also studied.

The proposed method was tested with polynomial guiding curves. It can also be applied to the rational B-spline guiding curves. More control points need to be added along the guiding curve direction to control the error between the designed surface and the machined surface. Alternatively, the rational guiding curves can first be approximated with polynomial curves and then be used to design the surface for flank milling.

In addition, the proposed method can also be applied to other developed flank milling tool positioning methods for flank millable surface design. This surface design method opens the door for engineer to integrate doubly curved surfaces in design of impellers and other performance critical objects.

To model a surface that meets the design requirements, multiple passes of the tool may be required. Previous work [6, 16] used piecewise ruled surfaces to meet the design requirements. Each ruled surface was an approximation to the surface swept by a tool pass. Rather than approximate with a ruled surface, one could instead use our technique and create an NURBS surface in place of each ruled surface. This piecewise NURBS surface would then be an exact representation of the final machined surface. While there are still issues with using these piecewise surfaces for flank milling, these issues occur whether you use piecewise ruled surface or if you use our piecewise NURBS surface. The point is that using our method instead of the ruled surfaces gives an exact model of the machined part that enables the design engineer to construct a tool path for a surface that more accurately matches the design specifications.

Acknowledgments This research was funded in part by the Natural Sciences and Engineering Research Council of Canada (NSERCC) and Ontario Centre of Excellence (OCE).

References

1. Rubio W, Lagarrigue P, Dessein G, Pastor F (1998) Calculation of tool paths for a torus mill on free-form surfaces on five-axis machines with detection and elimination of interference. Int J Adv Manuf Technol 14:13–20
2. Marciniak K (1991) Geometric modelling for numerically controlled machining. Oxford University Press, Oxford, UK
3. Stute G, Storr A, Sielaff W (1979) NC programming of ruled surface for five axis machining. Ann CIRP 28(1):267–271
4. Liu X (1995) Five-axis NC cylindrical milling of sculptured surfaces. Computer Aided Design 27(12):887–894
5. Rehsteiner F, Renker HJ (1993) Collision-free five-axis milling of twisted ruled surfaces. CIRP Ann 42(1):457–461
6. Bohez ELJ, Senadhera SDR, Pole K, Duflou JR, Tar T (1997) A geometric modelling and five-axis machining algorithm for centrifugal impellers. J Manuf Syst 16(6):422–463
7. Tsay DM, Her MJ (2001) Accurate 5-axis machining of twisted ruled surfaces. J Manuf Sci Eng 123:734–738
8. Bedi S, Mann S, Menzel C (2003) Flank milling with flat end cutters. Computer Aided Design 35:293–300
9. Menzel C, Bedi S, Mann S (2004) Triple tangent flank milling of ruled surfaces. Comp Aided Des 36:289–296
10. Li CG, Bedi S, Mann S (2006) Flank milling of ruled surface with conical tools—an optimization approach. Int J Adv Manuf Technol 29(11–12):1115–1124
11. Li CG, Bedi S, Mann S (2006) Flank milling surface design with the least square approach. WSEAS Transact Math 7(5):844–852
12. Redonnet J-M, Rubio W, Dessein G (1998) Side milling of ruled surfaces: optimum positioning of the milling cutter and calculation of interference. Advanced Manufacturing Technology 14(7):459–465
13. Monies F, Redonnet J-M, Rubio W, Lagarrigue P (2000) Improved position of a conical mill for machining ruled surfaces: application to turbine blades. J Eng Manufac 214:625–634, Part B
14. Monies F, Rubio W, Redonnet J-M, Lagarrigue P (2001) Comparative study of interference caused by different position settings of a conical milling cutter on a ruled surface. Proceedings of the Institution of Mechanical Engineers. B JNL Eng Manufact 215(9):1305

15. Monies F, Felices JN, Rubio W, Redonnet J-M, Lagarrigue P (2002) Five-axis NC milling of ruled surface: optimal geometry of a conical tool. Int J Prod Res 40(12):2901–2922
16. Elber G, Fish R (1997) 5-Axis freeform surface milling using piecewise ruled surface approximation. ASME 119:383–387
17. Yang J, Abdel-Malek K (2005) Approximate swept volumes of NURBS surfaces or solids. Comp Aided Geom Des 22:1–26
18. Mann S, Bedi S (2001) Generalization of the imprint method to general surfaces of revolution for NC machining. Comp Aided Des 34:373–378
19. Li CG, Mann S, Bedi S (2005) Error measurements for flank milling. Comp Aided Des 37:1459–1468
20. Lartigue C, Duc E, Affouard A (2003) Tool path deformation in 5-axis flank milling using envelop surface. Comp Aided Des 35:375–382
21. Senatore J, Monies F, Redonnet J-M, Rubio W (2005) Analysis of improved positioning in five-axis ruled surface milling using envelop surface. Comp Aided Des 37:989–998
22. Farin G (2002) Curves and surfaces for computer-aided geometric design: a practical guide. Academic Press, New York, USA
23. Li CG, Bedi S, Mann S (2007) Flank millable surface design in 5-axis machining. International Conference on Smart Machining Systems. Gaithersburg, Maryland, USA.